An optical lever approach to photodetector measurements of the pickup-head flying height in an optical disk drive

2006 Meas. Sci. Technol. 17 2335

(http://iopscience.iop.org/0957-0233/17/8/040)

INSTITUTE OF PHYSICS PUBLISHING MEASUREMENT SCIENCE AND TECHNOLOGY

Meas. Sci. Technol. **17** (2006) 2335–2342 doi:10.1088/0957-0233/17/8/040

An optical lever approach to photodetector measurements of the pickup-head flying height in an optical disk drive

C C Hsiao, C Y Peng and T S Liu

Department of Mechanical Engineering, National Chiao Tung University, Hsinchu 30010, Taiwan, Republic of China

E-mail: tsliu@mail.nctu.edu.tw

Received 12 April 2006, in final form 23 June 2006
Published 20 July 2006
Online at stacks.iop.org/MST/17/2335

Abstract

In order to increase the storage capacity and the density of near-field optical disk drives, a flying pickup-head has to allow a slider to fly at a stable height above the disk surface with the use of near-field optics. Since both the precision of the track pitch and the flying height are of a nanometre scale, it is necessary to increase the motion accuracy of the pickup-head. In this study, a piezoelectric bender is used as an actuator of the pickup-head, and two quadrant photodetectors are used to sense the pickup-head displacement and the rotating disk deformation. Based on an optical lever method that magnifies a small displacement, the flying height variation of the pickup-head above the disk is measured. Further results show that using the proposed measurement method in the real-time control of flying height is feasible.

Keywords: optical lever, photodetector, pickup-head, disk drive

(Some figures in this article are in colour only in the electronic version)

1. Introduction

An effective approach to the measurement of small displacements is with the use of optics. Anssi and Juha [1] presented a displacement sensing method using quadrant detectors. Zhang and Cai [2] proposed a focusing error detection technique based on an astigmatic method, consisting of a laser diode, an objective lens, a half mirror plate, and a quadrant detector. Chung *et al* [3] used an eight-segment photodiode to reduce the cross-talk in the wobble signal and the offset of the track error signal.

An optical lever magnifies a small displacement and thus makes an accurate measurement of the displacement possible. Kikukawa *et al* [4] employed an optical lever concept to detect displacement for a 10 μm long cantilever. An optical lever has also been used for measuring forces in atomic force microscopes [5, 6]. In addition, a near-field optical microscope was developed using the optical lever method [7].

Due to the requirement for more storage capacity, high-density optical storage devices have already become a hot topic. Near-field optical disk drives (NFODD) [8] can achieve higher density data than Blu-ray disks. Unlike CD-Roms, DVD-Roms and Blu-ray, in which electric motors actuate a lens in focusing motion, a slider in the pickup-heads of NFODD flies above a rotating disk in a similar manner to hard disk drives. Accordingly, the measurement of the flying height of the pickup-heads becomes critical.

To sense the pickup-head flying height variation, this study develops a measurement system that contains two quadrant photodetectors for sensing, and two laser diodes for use as light sources. The photodetectors are used to sense the disk and pickup-head displacements. Servo control experiments are carried out based on an optical lever method that is developed to obtain the flying height variation.

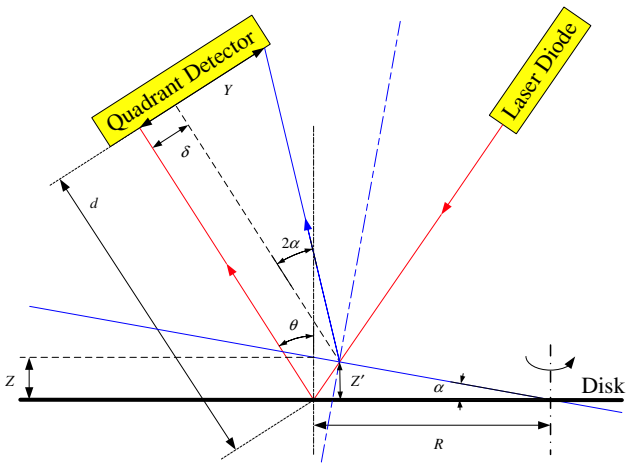

Figure 1. Schematic of the optical lever method where input displacement Z is amplified to become output Y.

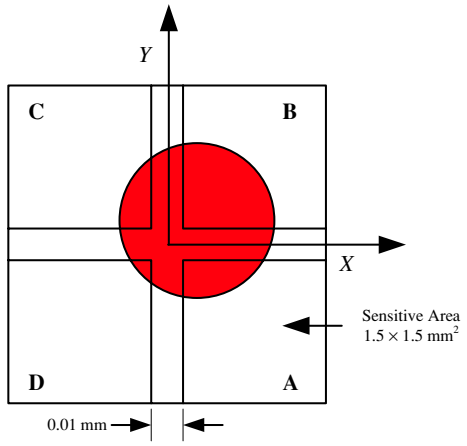

Figure 2. Quadrant detector.

2. Measurement system

The measurement system includes photodetectors, two laser diodes, and an op-amp circuit. Figure 1 depicts the measurement principle. The red line represents the laser beam that is first reflected from the disk surface and which then strikes a photodetector. However, when the disk surface deforms during rotation, the laser beam is reflected along a different path. The disk surface vibration causes the position of the beam spot on the photodetector to vary. An addition and subtraction operation in the op-amp circuits is carried out to deal with the output signals from the photodetectors. This study develops an optical lever method to obtain the relationship between the disk vibratory deformation and the variation of the laser spot position on the photodetector.

2.1. Photodetectors

To introduce the function of a photodetector, consider the example shown in figure 2, where a small, uniform, round spot of light strikes the detector. Symbols A, B, C and D denote the four quadrants of the photodetector. Each region denotes an individual photodiode. By comparing signals received from each of the four separate photodiodes, the spot position relative to the centre of the device can be determined. Specifically, X and Y displacements can be approximated as

$$X = \frac{(\mathrm{A}+\mathrm{B})-(\mathrm{C}+\mathrm{D})}{\mathrm{A}+\mathrm{B}+\mathrm{C}+\mathrm{D}}, \quad Y = \frac{(\mathrm{B}+\mathrm{C})-(\mathrm{A}+\mathrm{D})}{\mathrm{A}+\mathrm{B}+\mathrm{C}+\mathrm{D}}. \tag{1}$$

Some constraints have to be taken into account when using photodetectors for sensing displacement. Firstly, the spot of incident light must be smaller than the detector's total active area, but larger than the gap between individual active areas. Secondly, the total positional detection range is confined by both the spot size and to the detector's active area.

2.2. Optical lever method

The optical lever method is developed in this study to amplify the laser spot displacement and hence improve the sensing resolution. The present optical lever aims to amplify the input displacement Z to become the output displacement Y, as depicted in figure 1. From figure 3(*a*), using trigonometry yields

$$\tan\alpha = \frac{Z}{R}, \tag{2}$$

where α, Z and R denote the tilt angle of the disk surface, the disk deformation and the distance between the disk centre and the spot of the incident beam on the disk, respectively. From figure 3(*b*), using trigonometry yields

$$\varepsilon = \frac{\delta}{\cos\theta} \tag{3}$$

and

$$\tan\theta = \frac{\delta}{2Z'\cos\theta}, \tag{4}$$

where ε represents the length of a segment that is parallel to the disk surface before the disk deforms and is between the original incident and the reflected laser beam, δ is the distance from the intersection of the tilt disk and the incident laser to the original reflected light, θ is the incident angle and Z' is the distance from the intersection of the tilt disk and the incident laser to the original disk position. From figure 3(*c*), using trigonometry yields

$$Z = Z' + \frac{\varepsilon}{2}\tan\alpha. \tag{5}$$

Substituting equations (3) and (4) into equation (5) yields

$$\begin{aligned} Z &= Z' + \frac{2Z'\sin\theta}{2\cos\theta}\tan\alpha \\ &= Z'(1+\tan\theta\tan\alpha). \end{aligned} \tag{6}$$

Similarly, figure 3(*d*) gives

$$\tan 2\alpha = \frac{Y-\delta}{d-\frac{\delta}{\tan 2\theta}}, \tag{7}$$

where d represents the length of travel of the reflected beam to the photodetector before the disk deforms. Substituting equations (2), (3), (4) and (6) into equation (7) yields

$$\tan 2\alpha = \frac{Y-2\frac{Z\sin\theta}{1+\tan\theta\tan\alpha}}{d-2\frac{Z\sin\theta}{\tan 2\theta(1+\tan\theta\tan\alpha)}} = \frac{2\frac{Z}{R}}{1-\left(\frac{Z}{R}\right)^2}. \tag{8}$$

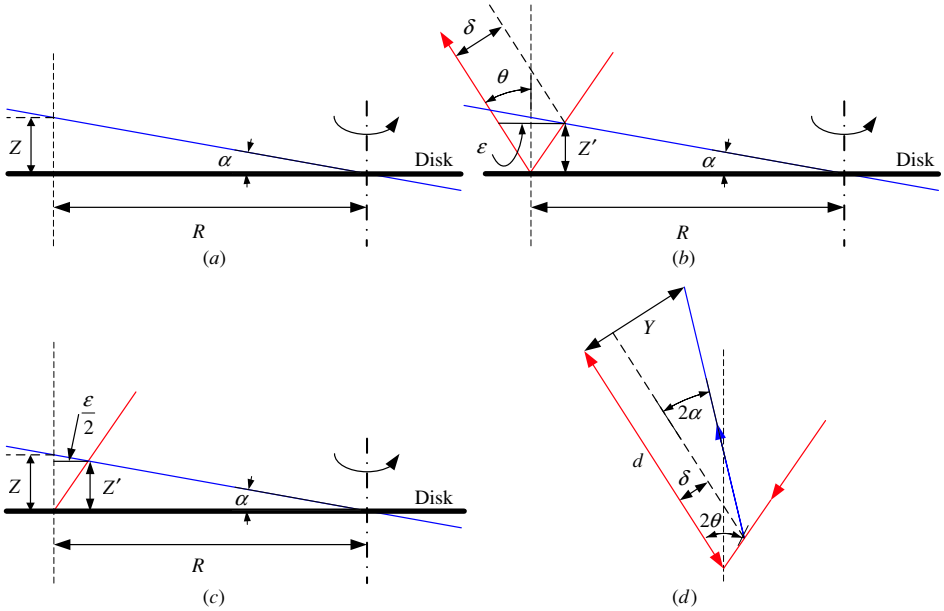

Figure 3. Geometry of the optical lever method with disk tilt angle α and incident angle θ: (*a*) disk deformation Z at distance R from disk centre, (*b*) disk deformation Z' at distance $R - \varepsilon/2$ from disk centre, (*c*) comparison between Z and Z' and (*d*) laser beam displacement Y on photodetector resulting from disk deformation.

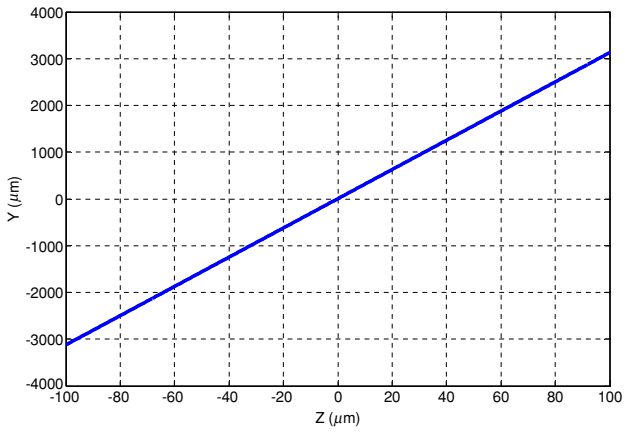

Figure 4. Relationship between the Y and Z displacements.

Equation (8) can be rearranged to

$$Y = \frac{2\frac{Z}{R}}{1-\left(\frac{Z}{R}\right)^2}\left(d - 2\frac{Z\sin\theta}{\tan 2\theta\left(1+\frac{Z}{R}\tan\theta\right)}\right) + \frac{2Z\sin\theta}{1+\frac{Z}{R}\tan\theta}. \tag{9}$$

Equation (9) relates the disk deformation Z to the beam spot displacement Y on the detectors. Since, in practice, R is much larger than Z, equation (9) can be reduced to $Y = 2\,\mathrm{d}Z/R$, which is a linear equation. Figure 4 depicts the linear relationship between Y and Z with a constant slope, i.e. the optical lever sensitivity is equal to 31.25. Based on this ratio, the disk deformation can be calculated from the photodetector signal. In a similar manner, the head displacement can be calculated. As a consequence, head flying height variation can be obtained by subtracting the disk deformation from the head displacement.

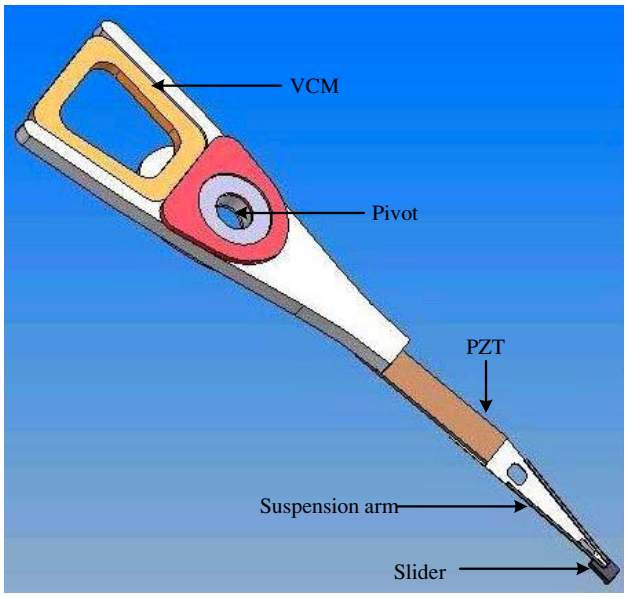

Figure 5. Pickup-head including the PZT bender.

3. Experiment

Piezoelectric (PZT) elements have been applied as actuators, and their performance is sufficient to generate fast and precise movement. Among the different PZT actuators [9–11], PZT benders are popular in many structure applications, such as the blade control of rotorcraft, vibration dampening, and positional control. In the presence of disk surface vibration, this study attaches a flying head with a PZT bender to a suspension arm in order to maintain a stable flying height, as depicted in figure 5.

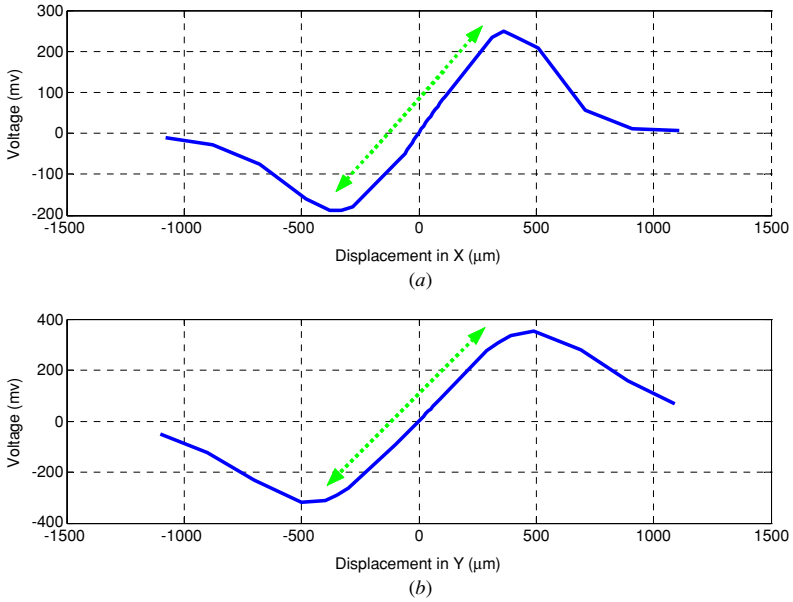

Figure 6. Measured linear range of the X and Y displacements.

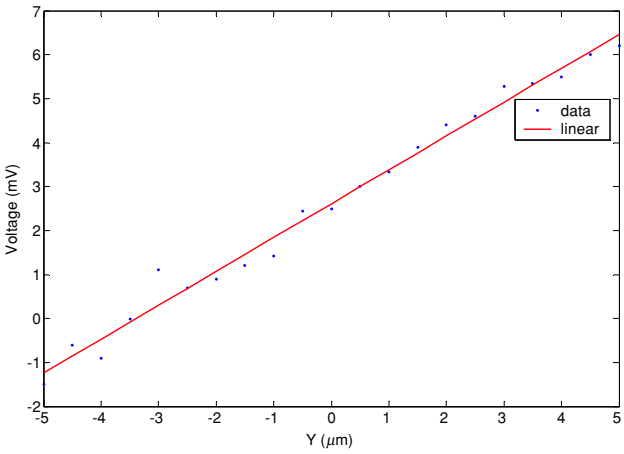

Figure 7. Resolution of the quadrant detector.

3.1. Photodetector measurements

Before measuring disk surface deformation, it is necessary to determine the linear ranges of the photodetector signals. In this experiment, a laser beam strikes the photodetector directly. The linear range of the photodetector is measured by moving a laser source fixed to an X–Y stage. Measurement results are shown in figure 6, where the horizontal axes are the X and Y displacements, and the vertical axes are the output voltages of the op-amp circuit. The linear range in both X and Y directions is about 650 μm.

Since the movement accuracy of the pickup-head is on a nanometre scale, the resolution of the measurements must also be on the same nanometre scale. The resolution of the photodetector is obtained by making the laser beam strike the detector directly, and then slowly moving the laser along the X direction of the detector. The manual movement step is 0.5 μm. As shown in figure 7, the horizontal and vertical axes represent the displacement in the Y direction and the output voltage of the photodetector, respectively. It is found that the resultant input–output relationship is linear. However, when the movement step is 0.4 μm, the resultant relationship becomes nonlinear, unlike figure 7. As a consequence, the resolution of the photodetector is 0.5 μm. Since this is not satisfactory, the resolution can be improved by using an optical lever method. According to equation (9), the ratio of Y (the beam varying spot displacement on the photodetector) to Z (the disk deformation) can be adjusted by modulating θ, R and d. However, the ratio is constrained to the measurable range of the photodetector and the disk surface deformation. It can be written as

$$\frac{Y_1}{Z_1} = \frac{Y_2}{Z_2}, \tag{10}$$

where $Y_1 = 0.5$ μm, $Y_2 = 650$ μm, Z_1, and Z_2 represent the resolution of the photodetector, the measurable range of the photodetector, the measurement resolution of the disk surface deformation, and the disk surface deformation respectively. A smaller Z_2 results in a finer Z_1; i.e. a smaller disk surface deformation generates a higher resolution in the disk deformation measurement. Since $Y_1 = 0.5$ μm and $Y_2 = 650$ μm, equation (10) leads to a linear relation between Z_2 and Z_1, i.e.

$$Z_2 = 1300 Z_1. \tag{11}$$

This study then uses a laser Doppler interferometer (LDV) [12, 13] to detect the disk surface deformation at different tracks and different rotation speeds. Figure 8 depicts the disk deformation at different radial positions of 2, 2.9 and 4.8 cm and disk rotation speeds of 1200, 3600 and 5400 rpm. The horizontal axis represents the distance between the disk centre and the measurement spot. Disk deformation attenuates with slower disk speed and spots closer to the disk centre. The disk speed prescribed at 1200 rpm and a laser beam position at a radial distance of 2.9 cm in this experiment results in a small deformation of 17 μm. Let Z_2 equal 20 μm, which

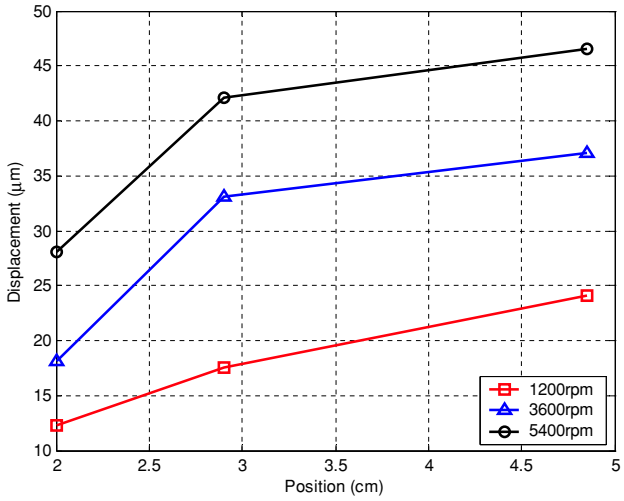

Figure 8. Disk surface deformation at different radial positions and rotation speeds.

Table 1. Parameter values in the experimental setup.

	θ (degree)	R (cm)	d (cm)
For disk	60	2.75	40.6
For pickup-head	55	4.5	66.6

is larger than the disk deformation, then equation (11) gives $Z_1 = 15.38$ nm < 16 nm.

As a consequence, the resolution of disk surface deformation measurements reaches 16 nm based on equations (10) and (11), and hence the ratio of Y_1 to Z_1 is $0.5/0.016 = 31.25$. The specifications of the experimental setup are shown in table 1, which is based on equation (9). Accordingly, each 16 nm deformation (Z in equation (9)) on the disk surface corresponds to 0.5 μm displacement (Y in equation (9)) on the photodetector. Based on the ratio of 31.25, the maximum vibration of a disk is approximately 20 μm, corresponding to a displacement of 625 μm on the photodetector. The signal remains in the linear range of figure 6. The following sections do not consider the measurement resolution, but use LDV to measure the displacement signals and to compare differences between the two signals measured by LDV and the optical lever.

3.2. Measurement of rotating disk deformation and pickup-head displacement

An experimental setup is shown in figure 9 where two sets of lasers and photodetectors measure the pickup-head displacement and the disk deformation. Figure 10 compares sensor voltages that represent the disk deformation as measured by the LDV and the photodetector when the disk rotates at 90 Hz. There is little difference between both signals. In order to measure another laser beam striking the front end of a pickup-head, a 90 Hz sine wave voltage input is applied to a PZT bender. The LDV and optical lever are used to measure the displacement of the pickup-head at the same time, and the result is shown in figure 11. Both results are consistent. Therefore, the measurement accuracy of the photodetector is validated.

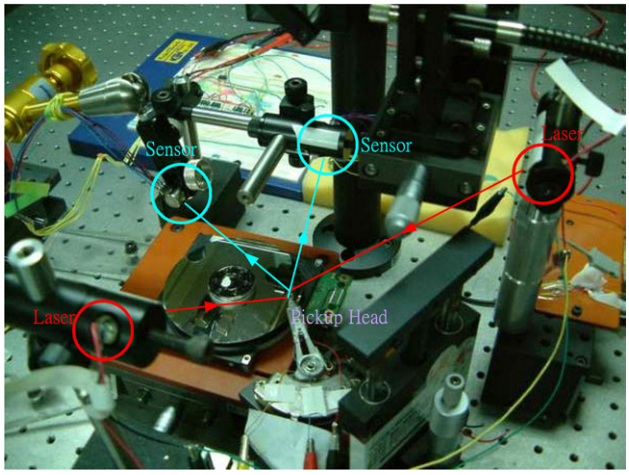

Figure 9. Experimental setup.

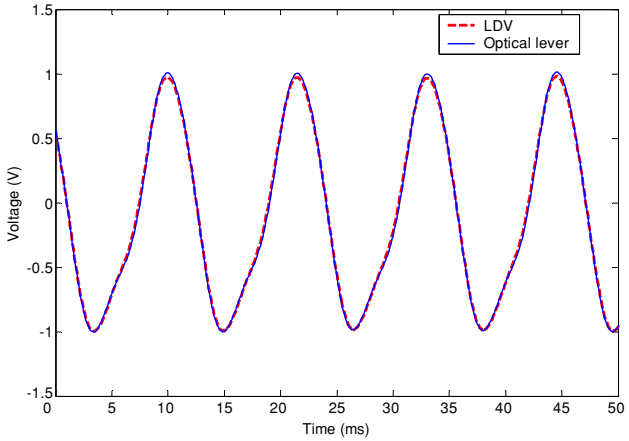

Figure 10. Disk surface vibrations measured by LDV and optical lever.

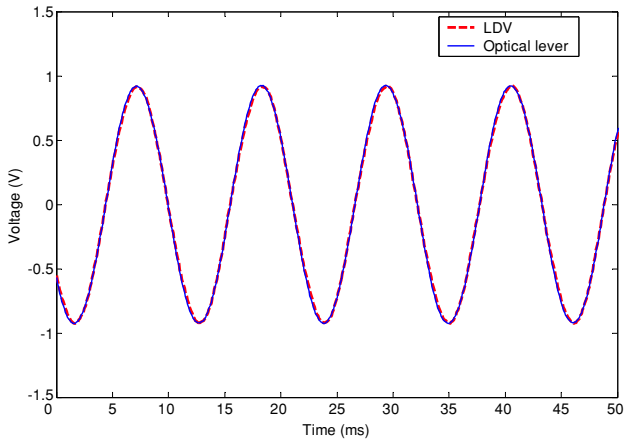

Figure 11. Pickup-head displacements measured by LDV and optical lever.

3.3. Flying height measurement

A PC-based experimental setup is constructed as depicted in figure 12. The experimental setup consists of a disk, a variable speed motor, two photodetectors and two red-ray laser diodes,

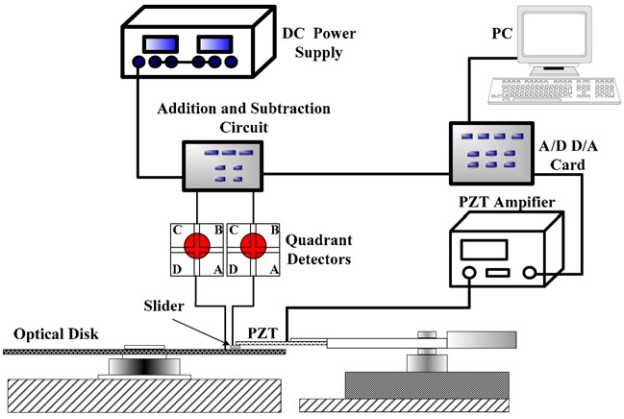

Figure 12. Schematic diagram of the experimental setup.

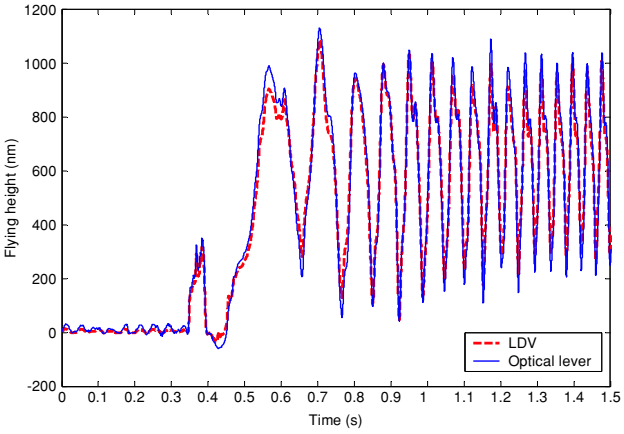

Figure 13. Comparison of measured flying heights using LDV and optical lever.

a dual-beam LDV, and a pickup-head based on the parameters given in table 1. Figure 13 depicts the flying height of the pickup-head measured by the LDV and the optical lever. The difference between the LDV and optical lever results are small, and are of a manner similar to figures 10 and 11. The disk does not rotate until a time of 0.346 s, and the pickup-head takes off from the disk surface at 0.451 s. Therefore, it takes 0.105 s to overcome the preload of the suspension before take-off. The pickup-head flies stably after 1 s. The flying height varies between 120 and 1080 nm and therefore has a variation of 960 nm.

4. Control experiment

This study carries out head flying height control so that the PZT actuator can track the disk surface deformation. System identification is carried out by applying a known control voltage that results in bender displacement. With the LDV as a sensor, the system identification procedure leads to a PZT bender transfer function that relates control voltage to bender displacement, i.e.

$$\frac{Y(s)}{U(s)} = \frac{1.779 \times 10^8 s^2 + 2.055 \times 10^{10} s + 1.886 \times 10^{15}}{s^4 + 1203 s^3 + 1.047 \times 10^8 + 2.657 \times 10^{10} + 4.235 \times 10^{14}}. \quad (12)$$

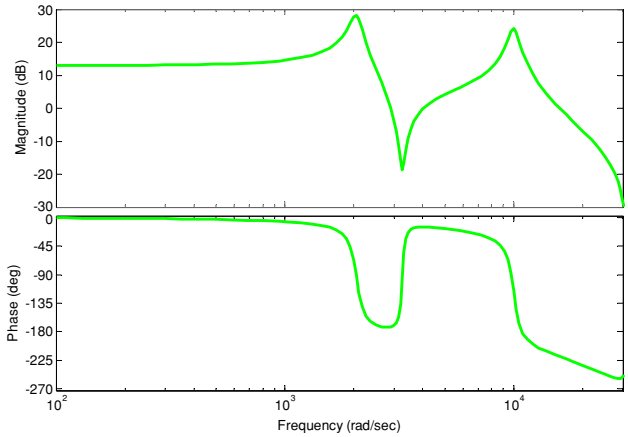

Figure 14. Bode plot of PZT model.

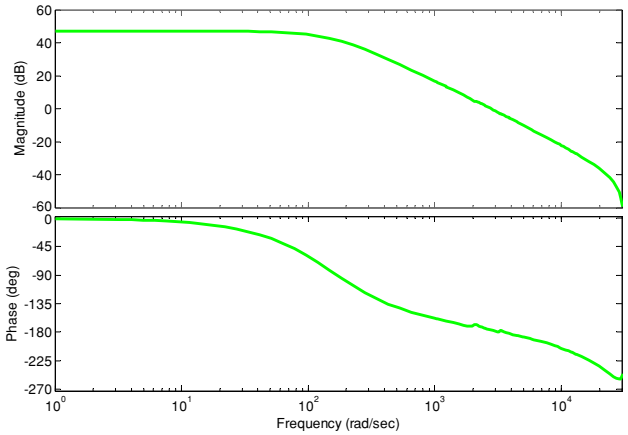

Figure 15. Bode plot with compensator included.

Equation (12) is the continuous-time model of the PZT bender. Its Bode plot is shown in figure 14, which presents a stable system. At sampling times of 0.1 ms, equation (12) can be written in a discrete form

$$\frac{Y(z)}{U(z)} = \frac{0.7935z^3 - 0.7306z^2 - 0.656z + 0.7557}{z^4 - 2.965z^3 + 3.877z^2 - 2.762z + 0.8867}. \quad (13)$$

According to figure 14, two resonances exist at 2×10^3 and 10×10^3 rad s^{-1}. Since resonances may cause a divergence in the control, a compensator, consisting of two notch filters, is designed to suppress both resonances. The compensator is expressed by

$$C(z) = \frac{0.05(z - 0.9233)(z^2 - 1.938z + 0.9794)(z^2 - 1.027z + 0.9057)}{(z - 0.9)(z^2 - 1.97z + 0.9702)(z^2 - 1.883z + 0.9878)}. \quad (14)$$

Equations (13) and (14) constitute a compensated system. Figure 15 depicts the Bode plot after compensation, when both resonances have been suppressed. As can be seen, the dynamics of the compensated system is better than that without compensation.

This experiment deals with a flying pickup-head in NFODD that uses a PZT bender as an actuator, and whose design was shown in figure 5. Since a large deformation

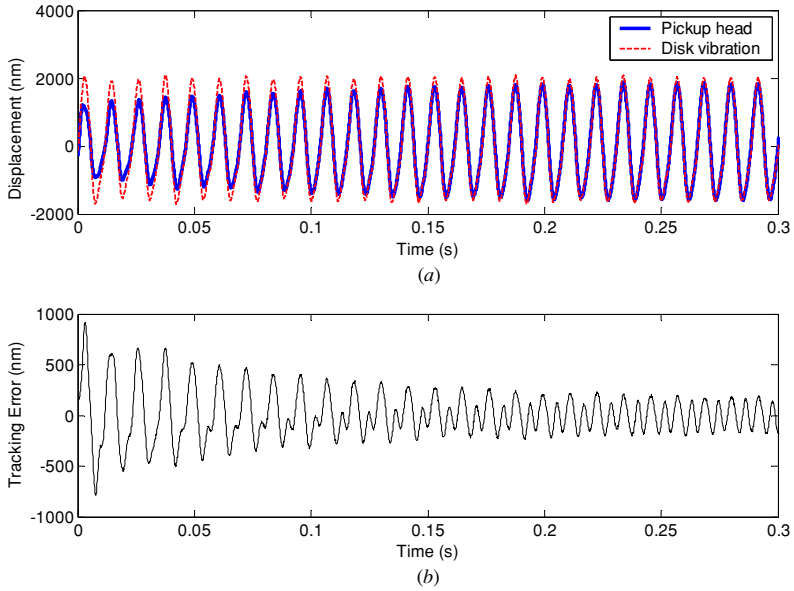

Figure 16. Control result of (*a*) pickup-head tracking disk surface vibration and (*b*) tracking error.

of the disk surface during disk rotation may well degrade focusing performance in near-field disk drives, in the present pickup-head the PZT bender is attached to a suspension arm. The PZT bender enables the pickup-head to maintain a stable flying height. Two photodetectors and two red-ray laser diodes measure variations of the disk surface deformation and the pickup-head flying height.

The disk rotates at 90 Hz in this control experiment. Figure 16 depicts the disk surface deformation and pickup-head displacement, and tracking error. The disk deformation and tracking error are approximately 3700 and 360 nm respectively. The steady state error lies within 9.7%, and the convergence time is about 0.3 s.

5. Conclusions

Based on the optical lever method, this study measures the flying height of a PZT bender that serves as a fine actuator in the pickup-head for focusing motion. Moreover, a control experiment results in a tracking error that is within 9.7% of the experiments.

According to figure 6, the useful measurement range of a photodetector is about 650 μm in both the X and Y displacements. By using photodetectors and the optical lever method, the sensing resolution of the disk surface deformation and the pickup-head flying height variation can reach 16 nm, while the disk surface deformation gains 20 μm. According to measurement results for a disk spinning at 20 Hz, a 1 V signal detected by the photodetector corresponds to a 8 μm displacement measured by the LDV.

The optical lever method, LDV and the gap capacitance method [14] all can be used to measure tiny displacements in motion. However, LDV is the most expensive in experimental measurement setups. Both the optical lever method and LDV can obtain nanometre precision, whereas the gap capacitance method only obtains sub-micrometre or micrometer precision. Further, the gap capacitance method only applies to objects with a metal surface. Hence, the optical lever method is promising for the measurement of tiny displacements.

Acknowledgment

The authors gratefully acknowledge the support of the 'Pursuing Academic Excellence Project' of the National Science Council and Department of Education in Taiwan, ROC, under grant no NSC93–2752-E009–009-PAE.

References

[1] Anssi J M and Juha T K 1995 A high-resolution lateral displacement sensing method using active illumination of a cooperative target and a focused four-quadrant position-sensitive detector *IEEE Trans. Instrum. Meas.* **44** 46–52

[2] Zhang J and Cai L 1996 A compact optical vibration transducer with photo IC *IEEE Instrum. Meas. Technol. Conf. (Brussels, Belgium)* pp 513–7

[3] Chung C S, Ahn Y, Kim T K, Ma B I, Lee K G and Park I S 2003 One beam optical head for high-density optical system with eight segment photodiode *Japan. J. Appl. Phys.* 1 **42** 908–11

[4] Kikukawa A, Koyanagi H, Etoh K and Hosaka S 2000 In-line optical lever system for ultrasmall cantilever displacement detection *Japan. J. Appl. Phys.* 1 **39** 1885–9

[5] Fujisawa S, Ohta M, Konishi T, Sugawara Y and Morita S 1994 Difference between the forces measured by an optical lever deflection and by an optical interferometer in an atomic force microscope *Rev. Sci. Instrum.* **65** 644–7

[6] Higgins M J, Proksch R, Sader J E, Polcik M, Mc Endoo S, Cleveland J P and Jarvis S P 2006 Noninvasive determination of optical lever sensitivity in atomic force microscopy *Rev. Sci. Instrum.* **77** 013701–5

[7] Ono M, Sone H and Hosakas S 2005 Prototype of atomic force cantilevered SNOM based on through-the-lens-type optical lever and polarized illumination and detection system *Japan. J. Appl. Phys.* **44** 5434–7

[8] Milster T D 2000 Near-field optics: a new tool for data storage *Proc. IEEE* **88** 1480–90
[9] Jenkins D F L, Chilumbu C, Tunstall G, Clegg W W and Robinson P 2001 Multi-layer bulk PZT actuators for flying height control in ruggedised hard disk drives *IEEE Int. Symp. Appl. Ferroelectr.* **1** 293–6
[10] Tsaur J, Zhang L, Maeda R, Matsumoto S and Khumpuang S 2002 Design and fabrication of 1D and 2D micro scanners actuated by double layered lead zirconate titanate (PZT) bimorph beams *Japan. J. Appl. Phys.* 1 **41** 4321–6
[11] Cappelleri D J, Frecker M I and Simpson T W 2000 Optimal design of a PZT bimorph actuator for minimally invasive surgery *Proc. SPIE Int. Soc. Opt. Eng.* **3984** 321–35
[12] Bruce R A 2004 Comparing dynamic surface tlt with velocity using an LDV *Proc. SPIE Int. Soc. Opt. Eng.* **5503** 347–57
[13] Stanbridge A B, Ind P R and Ewins D J 2004 Measuring vibration of cylindrical surfaces using a continuous-scan LDV *Proc. SPIE Int. Soc. Opt. Eng.* **5503** 249–59
[14] Chen J W and Liu T S 2004 A gap capacitance method for slider flying height measurement in near-field optical disk drives *Mechatronics* **14** 1141–5